

Measuring cosmic baryon density with FRB and GW data

JI-GUO ZHANG,¹ JI-YU SONG,¹ ZE-WEI ZHAO,² WAN-PENG SUN,¹ JING-FEI ZHANG,¹ AND XIN ZHANG^{1,3,4}

¹Key Laboratory of Cosmology and Astrophysics (Liaoning Province) & Department of Physics, College of Sciences, Northeastern University, Shenyang 110819, People's Republic of China

²Department of Biomedical Engineering, School of Medical Devices, Shenyang Pharmaceutical University, Shenyang 110016, People's Republic of China

³Key Laboratory of Data Analytics and Optimization for Smart Industry (Ministry of Education), Northeastern University, Shenyang 110819, People's Republic of China

⁴National Frontiers Science Center for Industrial Intelligence and Systems Optimization, Northeastern University, Shenyang 110819, People's Republic of China

ABSTRACT

The dispersion measure (DM) analysis of extragalactic fast radio bursts (FRBs) has accounted for all cosmic baryons but remains limited by systematic uncertainties from various parameter degeneracies. We show that the prominent degeneracy between the baryon density (Ω_b) and the Hubble constant (H_0) can be disentangled through an independent H_0 value uniquely inferred from the absolute luminosity distance measurements of gravitational-wave (GW) standard sirens. By combining 104 localized FRBs with 47 GW events, we obtain a robust, late-Universe measurement of $\Omega_b = 0.0488 \pm 0.0064$ (1σ), in concordance with early-Universe observations of CMB + BBN. Notably, incorporating GW data helps not only avoid biases induced by the H_0 tension, but also mitigate those from the parameters of diffuse baryon fraction and DM distribution models. Although the current precision ($\sim 13\%$) is limited by sample size, the growing detections of both FRBs and GWs will make their synergy a powerful probe of low-redshift cosmology.

Keywords: Cosmological parameters (339); Baryon density (139); Radio bursts (1339); Gravitational waves (678)

1. INTRODUCTION

The concordance cosmology predicts consistency among independent probes across all epochs (Ostriker & Steinhardt 1995). However, while the cosmic microwave background (CMB) and Big Bang nucleosynthesis (BBN) provide precise estimates of the baryon content in the early Universe (Cooke et al. 2018), about 30% baryons remain undetected in the local Universe (Shull et al. 2012). These missing baryons are thought to reside in diffuse ionized gas that is too faint to be directly observed, known as the “missing baryon problem” (Fukugita et al. 1998; Cen & Ostriker 1999).

Fast radio bursts (FRBs) are bright, millisecond-duration radio transients of extragalactic origin (Lorimer et al. 2007; Thornton et al. 2013). Their observed dispersion measures (DMs) trace the integrated column density of free electrons along the line of sight (LoS), making them sensitive to baryons in the intergalactic medium (IGM) (McQuinn 2013). Thus, FRBs with known redshifts derived from pre-

cise host galaxy localization can be used to trace the missing baryons (Deng & Zhang 2014; Connor et al. 2025). Macquart et al. (2020) (hereafter Macquart20) first employed 5 localized FRBs to estimate the present-day cosmic baryon density of $\Omega_b = 0.051^{+0.021}_{-0.020}$ at the 95% confidence level, which agrees with the joint CMB and BBN result and likely resolves the local baryon problem. Yang et al. (2022) (hereafter Yang22) used an updated sample of 22 localized FRBs and obtained $\Omega_b = 0.0490^{+0.0036}_{-0.0033}$ at the 1σ level, reinforcing the evidence for a complete cosmic baryon census. With the high event rate and increasing number of localized events, FRBs have emerged as a promising cosmological probe (Zhou et al. 2014; Gao et al. 2014); see Bhandari & Flynn (2021), Wu & Wang (2024), and Glowacki & Lee (2025) for recent reviews.

However, FRB cosmology based on DM is hindered by parameter degeneracies, which result in two main sources of systematic uncertainties (Kumar & Linder 2019). The first is from extracting the IGM contribution (DM_{IGM}) from the total DM budget (see Eq. (1)). This is mainly due to the difficulty in modeling both the host contribution (DM_{host}) and the LoS inhomogeneity in the IGM. Macquart20 modeled their probability distributions and Zhang et al. (2020,

2021) further employed the IllustrisTNG simulations to derive priors on these empirical DM model parameters for different FRB populations, which effectively reduce biases induced by host galaxy diversity and IGM fluctuations. However, the second uncertainty from the analysis of the extracted DM_{IGM} remains challenging to control. This is because its redshift relation (known as the Macquart relation) exhibits intrinsic degeneracies among Ω_b , the Hubble constant (H_0), and the baryon fraction in diffuse ionized gas (f_d) (see Eq. (3)). Given the limited constraints on f_d , it is commonly modeled as either a constant or a redshift-dependent function in the literature (Li et al. 2020; Qiang & Wei 2020; Wang & Wei 2023; Liu et al. 2025). Although H_0 has been precisely measured, estimates from early- (e.g., Planck 2018 CMB (Aghanim et al. 2020) (hereafter Planck18)) and late-Universe (e.g., SH0ES Cepheid-calibrated Type Ia supernovae (SNe) (Riess et al. 2022)) observations show a significant discrepancy now exceeding 5σ , which has widely been known as the “ H_0 tension” (Guo et al. 2019; Di Valentino et al. 2021; Abdalla et al. 2022; Hu & Wang 2023). This inconsistency would introduce systematic uncertainties into the estimation of Ω_b using FRB samples. It should be noted that Macquart20 and Yang22 derived their respective estimates of Ω_b by assuming $H_0 = 70 \text{ km s}^{-1} \text{ Mpc}^{-1}$ and a flat prior over $67\text{--}74 \text{ km s}^{-1} \text{ Mpc}^{-1}$, which provides a reasonable strategy for handling the second uncertainty given the H_0 tension (note that many studies also constrain H_0 by adopting early-Universe priors on $\Omega_b h^2$; see, e.g., Hagstotz et al. (2022)). Alternatively, jointly analyzing FRBs and datasets that independently measure H_0 would also be welcome.

As an emerging cosmological probe, gravitational-wave (GW) standard sirens offer unique advantages for measuring H_0 (Schutz 1986). This primarily arises from the fact that the amplitudes of GW waveforms are inversely proportional to the luminosity distances (D_L) to the sources, allowing for a direct measurement of D_L through waveform analysis. Since $D_L \propto 1/H_0$, GW standard sirens serve as a powerful and self-calibrating probe for determining H_0 , provided that the redshifts of the GW sources are also known (Dalal et al. 2006; Cutler & Holz 2009; Zhao et al. 2011; Cai & Yang 2017; Abbott et al. 2017a,b,c; Chen et al. 2018; Cai et al. 2018; Wang et al. 2018; Zhang et al. 2019a,b; Zhang 2019; Wang et al. 2020; Zhao et al. 2020b; Gray et al. 2020; Jin et al. 2020; Yu et al. 2020; Wang et al. 2022; Zhu et al. 2022a,b; Wu et al. 2023; Muttoni et al. 2023; Yun et al. 2023; Yu et al. 2024; Han et al. 2024; Feng et al. 2024; Song et al. 2024; Jin et al. 2024a,b; Li et al. 2024; Dong et al. 2024; Xiao et al. 2024; Zhu et al. 2024; Zheng et al. 2024; Han et al. 2025). During the first three observing runs of the LIGO, Virgo, and KAGRA (LVK) collaboration, approximately 100 GW events were detected and collected in the third Gravitational-Wave Transient Catalog (GWTC-3). Us-

ing 47 high-signal-to-noise ratio (SNR) GW standard sirens from GWTC-3, Abbott et al. (2023a) obtained a $\sim 10\%$ precision on H_0 . Song et al. (2025) further combined these 47 GW standard sirens with an additional strong lensing system and achieved a model-independent constraint on H_0 with a precision of $\sim 8\%$. Therefore, the H_0 information uniquely provided by GW data enables a direct estimate of Ω_b disentangled from H_0 in the Macquart relation, which offers new insight into resolving systematic effects in FRB cosmology.

Unlike previous studies that combined FRBs with traditional observations such as SNe (Jaroszynski 2019; Gao et al. 2023) or CMB (Zhao et al. 2020a; Qiu et al. 2022), we highlight that combining with GWs inherently involves calibration-free distances and avoids reliance on early-time physics. More recently, Zhang & Zhang (2025) and Gao et al. (2025b) proposed a novel method based on FRB/persistent radio sources (PRS) associations, which awaits the detection of more such events. The FRB + GW synergy is promising, with numerous detections expected from both communities in next-generation surveys (Zhang et al. 2023).

In this Letter, we combine 104 localized FRBs with 47 GW events from the GWTC-3 catalog to jointly constrain Ω_b and H_0 , without relying on any cosmological priors. To control the aforementioned systematics, we allow all DM parameters¹ to vary freely and incorporate GW data to break parameter degeneracies. Note that we do not assume any FRB/GW associations (see Wei et al. (2018) and Qiang et al. (2025) for studies based on such associations).

2. DATA AND METHODOLOGY

2.1. Localized FRB data

In this section, we first present the likelihood function for localized FRBs based on DM analysis following Macquart20, then the FRB sample used in this work.

The observed dispersion measure can be decomposed into several components:

$$\text{DM}_{\text{obs}} = \text{DM}_{\text{MW,ISM}} + \text{DM}_{\text{MW,halo}} + \text{DM}_{\text{IGM}} + \text{DM}_{\text{host}}, \quad (1)$$

where the Milky Way contribution includes the interstellar medium (ISM) contribution $\text{DM}_{\text{MW,ISM}}$ estimated from the electron density models such as NE2001 (Cordes & Lazio 2002), based on the source coordinates. The halo contribution of the Milky Way ($\text{DM}_{\text{MW,halo}}$) is estimated to lie in the range $50\text{--}80 \text{ pc cm}^{-3}$ (Prochaska & Zheng 2019). Thus, we assume a Gaussian distribution $P_{\text{halo}}(\text{DM}_{\text{halo}})$ with the mean value of $\mu_{\text{halo}} = 65 \text{ pc cm}^{-3}$ and standard deviation

¹ In this context, we refer to the DM parameters as $(f_d, F, \mu_{\text{host}}, \text{and } \sigma_{\text{host}})$, while the empirical DM model parameters refer specifically to $(F, \mu_{\text{host}}, \text{and } \sigma_{\text{host}})$. The parameters are defined in Sec. 2.1.

of $\sigma_{\text{halo}} = 25 \text{ pc cm}^{-3}$ (Yang et al. 2022)), i.e.,

$$P_{\text{halo}}(\text{DM}_{\text{halo}}) = \frac{1}{\sqrt{2\pi}\sigma_{\text{halo}}} \exp \left[-\frac{(\text{DM}_{\text{halo}} - \mu_{\text{halo}})^2}{2\sigma_{\text{halo}}^2} \right]. \quad (2)$$

The average DM_{IGM} in the standard ΛCDM (cosmological constant Λ + cold dark matter) cosmology is given by the Macquart relation,

$$\langle \text{DM}_{\text{IGM}} \rangle = \frac{3cf_e}{8\pi G m_p} \Omega_b H_0 f_d \int_0^z \frac{(1+z)dz}{\sqrt{\Omega_m(1+z)^3 + (1-\Omega_m)}}, \quad (3)$$

where Ω_m is the present matter density parameter, c is the speed of light, G is the gravitational constant, m_p is the proton mass, and f_e is the number of ionized electrons per baryon, which can be approximated as 7/8 for $z < 3$.

The IGM plasma is inhomogeneous, and the true value of DM_{IGM} would vary significantly around the mean value $\langle \text{DM}_{\text{IGM}} \rangle$ due to the LoS variance caused by intersecting foreground galaxy halos. Thus, the probability distribution of DM_{IGM} is

$$P_{\text{IGM}}(\Delta) = A\Delta^{-\beta} \exp \left[-\frac{(\Delta^{-\alpha} - C_0)^2}{2\alpha^2\sigma_{\text{IGM}}^2} \right], \quad \Delta > 0, \quad (4)$$

where $\Delta \equiv \text{DM}_{\text{IGM}} / \langle \text{DM}_{\text{IGM}} \rangle$. α and β , which describe the inner gas density profile of halos, are best fitted as $\alpha = 3$ and $\beta = 3$ according to hydrodynamic simulations. The effective standard deviation $\sigma_{\text{IGM}} = Fz^{-1/2}$ is parameterized by Macquart20, where F is the parameter reflecting the galactic feedback. Here, A is a normalization constant, and C_0 is chosen to ensure that the mean of this distribution is unity. Note that we include the factor $1/\langle \text{DM}_{\text{IGM}} \rangle$ suggested by (Zhang et al. 2025b) when normalizing Eq. (4).

The distribution of DM_{host} is modeled as

$$P_{\text{host}}(\text{DM}_{\text{host}}) = \frac{1}{\sqrt{2\pi}\sigma_{\text{host}}\text{DM}_{\text{host}}} \times \exp \left[-\frac{(\ln \text{DM}_{\text{host}} - \mu_{\text{host}})^2}{2\sigma_{\text{host}}^2} \right], \quad (5)$$

where a correction $\text{DM}_{\text{host}} \rightarrow \text{DM}_{\text{host}}/(1+z)$ has been applied. The mean value and variance of the distribution are $e^{\mu_{\text{host}}}$ and $e^{2\mu_{\text{host}}+\sigma_{\text{host}}^2}(e^{\sigma_{\text{host}}^2}-1)$, respectively.

Thus, the total likelihood of the localized FRB data set $\{x_{\text{FRB}}\}$ composed of N_{FRB} sources, is given by

$$\mathcal{L}_{\text{FRB}}(\{x_{\text{FRB}}\}) = \sum_{i=1}^{N_{\text{FRB}}} P_i(\text{DM}'_i). \quad (6)$$

For the i -th FRB, the possibility distribution of its extragalactic DM component ($\text{DM}' = \text{DM}_{\text{IGM}} + \text{DM}_{\text{host}}$) is computed

by convolving Eqs. (2), (4), and (5):

$$P_i(\text{DM}'_i) = \int_{30 \text{ pc cm}^{-3}}^{100 \text{ pc cm}^{-3}} P_{\text{halo}}(\text{DM}_{\text{halo}}) d\text{DM}_{\text{halo}} \times \int_0^{\text{DM}'_i - \text{DM}_{\text{halo}}} P_{\text{host}}(\text{DM}_{\text{host}}) \times P_{\text{IGM}}(\text{DM}'_i - \text{DM}_{\text{halo}} - \text{DM}_{\text{host}}) d\text{DM}_{\text{host}}. \quad (7)$$

We also consider a scenario in which the empirical DM model parameters are fixed, though our main results treat them as free. Specifically, we adopt values calibrated from cosmological hydrodynamical simulations, notably the IllustrisTNG simulation, which provides redshift-dependent distributions for both $P_{\text{IGM}}(\text{DM}_{\text{IGM}})$ (Zhang et al. 2021) and $P_{\text{host}}(\text{DM}_{\text{host}})$ (Zhang et al. 2020). The parameters $A(z)$, $C_0(z)$, and $\sigma_{\text{IGM}}(z)$ in Eq. (4), as well as $\mu_{\text{host}}(z)$ and $\sigma_{\text{host}}(z)$ in Eq. (5), are interpolated from best-fit simulation results across redshift. Note that μ_{host} and σ_{host} are further fixed based on the host galaxy types (see the seventh column of Table 2).

Finally, we select a sample of 104 localized FRBs from an initial set of 119, based on the following criteria: (1) $\text{DM}_{\text{MW,ISM}}$ is required to be less than 40% of DM_{obs} (Connor et al. 2025); (2) $\text{DM}_{\text{obs}} - \text{DM}_{\text{MW,ISM}}$ is taken to exceed 80 pc cm^{-3} , ensuring a positive DM_{host} ; (3) FRB 20190520B and FRB 20220831A are excluded due to excess local DM contributions from their host environments. The final sample is listed in Appendix B (see Table 2).

2.2. GW standard siren data

We use 47 GW standard sirens with SNRs greater than 11 and an inverse false alarm rate exceeding 4 yr from GWTC-3, covering a redshift range of approximately $z < 0.8$. The sample consists of 42 BBHs, three neutron star-black holes (NSBHs), and two binary neutron stars (BNSs).

We obtain the redshift of GW170817 from the electromagnetic (EM) counterpart (Abbott et al. 2017a,b,c). For GW events without EM counterparts, we obtain their redshifts through the dark siren method (Schutz 1986; Mastrogiovanni et al. 2023; Gray et al. 2023) and incorporate the GLADE+ catalog (Dálya et al. 2022). In the following, we provide a brief introduction to the likelihood function of GW standard sirens. We denote the source parameters of each GW event by θ , and the population-level parameters by Λ , including population model parameters and cosmological parameters. For GW events without EM counterparts, assuming a “scale-free” prior on the expected number of detected events N_{exp} , i.e., $\pi(N_{\text{exp}}) \propto 1/N_{\text{exp}}$, the likelihood function of the GW data set $\{x_{\text{GW}}\}$ composed of N_{GW} GW events (Mastrogiovanni et al. 2023) is

vanni et al. 2021; Abbott et al. 2023b), is given by

$$\mathcal{L}_{\text{GW}}(\{x_{\text{GW}}\}|\boldsymbol{\Lambda}) \propto \prod_i^{N_{\text{GW}}} \frac{\int d\boldsymbol{\theta} \mathcal{L}(x_{\text{GW},i}|\boldsymbol{\theta}, \boldsymbol{\Lambda}) \frac{dN_{\text{CBC}}(\boldsymbol{\Lambda})}{d\boldsymbol{\theta} dt}}{\int d\boldsymbol{\theta} P_{\text{det}}(x_{\text{GW},i}|\boldsymbol{\theta}, \boldsymbol{\Lambda}) \frac{dN_{\text{CBC}}(\boldsymbol{\Lambda})}{d\boldsymbol{\theta} dt}}, \quad (8)$$

where $\mathcal{L}_{\text{GW}}(x_{\text{GW},i}|\boldsymbol{\theta}, \boldsymbol{\Lambda})$ is the parameter estimation likelihood, quantifying the uncertainties in measuring the GW source parameters $\boldsymbol{\theta}$ through waveform analysis. $dN_{\text{CBC}}(\boldsymbol{\Lambda})/d\boldsymbol{\theta} dt$ is the CBC detection rate in the detector frame, which includes population models of GW sources, cosmological models, and redshift information from the GLADE+ galaxy catalog. In assessing the completeness of the GLADE+ catalog, we adopt a Schechter function to describe the B -band absolute magnitude distribution of galaxies (Kochanek et al. 2001). We further assume that the probability of a galaxy being the host of the GW source is proportional to its B -band luminosity. $P_{\text{det}}(x_{\text{GW},i}|\boldsymbol{\theta}, \boldsymbol{\Lambda})$ is the detection probability of a GW event with parameters of $\boldsymbol{\theta}$ and $\boldsymbol{\Lambda}$. The denominator of Eq. (8) accounts for the GW selection effect.

For GW dark sirens, population models can help infer redshift for the sources, especially in scenarios where the galaxy catalog is significantly incomplete (Taylor et al. 2012; Ezquiaga & Holz 2022; Mastrogiovanni et al. 2023; Gray et al. 2023). We adopt the same population model assumptions as Abbott et al. (2023a), but restrict our analysis to the Power Law + Peak BBH mass model, which is best supported by the data. Considering additional models would increase computational cost and lies beyond the scope of this work. For BNSs, we assume that neutron star masses are uniformly distributed in the range of $1\text{--}3 M_\odot$. In the case of NSBH systems, the black hole component is drawn from the same distribution as the primary black holes in BBHs, while the neutron star component follows the mass distribution assumed for BNSs. The redshift distribution of GW sources is modeled using a phenomenological prescription that traces the cosmic star formation rate. Consistent with Abbott et al. (2023a), we disregard potential redshift evolution in the BBH mass distribution as well as variations in the GW detection rate arising from the spin distribution. These effects are currently subdominant compared to the statistical uncertainties present in the existing GW observations.

In cases where EM counterparts are detected, the information from EM observations should be incorporated alongside GW data. Since GW and EM detections are statistically independent, the overall likelihood is given by

$$\mathcal{L}_{\text{EM+GW}}(x_{\text{GW},i}|\boldsymbol{\theta}) \propto \mathcal{L}_{\text{EM}}(x_{\text{GW},i}|z, \Omega) \mathcal{L}_{\text{GW}}(x_{\text{GW},i}|\boldsymbol{\theta}), \quad (9)$$

where $\mathcal{L}_{\text{EM}}(x_{\text{GW},i}|z, \Omega)$ quantifies the measurement uncertainties of the redshift z and the sky localization Ω from EM observations. We assume that the probability of having EM observations is 1 once an EM counterpart is present (Gray

et al. 2020; Mastrogiovanni et al. 2024). This assumption holds only within the current GW detection range, as it remains much smaller than that of EM observations.

2.3. Joint analysis of FRB and GW data

We jointly constrain cosmological and FRB-related DM parameters, and adopt flat priors for the following seven parameters: $\Omega_m \in \mathcal{U}(0.28, 0.35)$ (Yang et al. 2022), $\Omega_b \in \mathcal{U}(0.01, 0.10)$, $H_0 \in \mathcal{U}(20, 140) \text{ km s}^{-1} \text{ Mpc}^{-1}$, $f_d \in \mathcal{U}(0.84, 0.96)$,² $F \in \mathcal{U}(0.011, 1.0)$, $\mu_{\text{host}} \in \mathcal{U}(3.0, 5.3)$, and $\sigma_{\text{host}} \in \mathcal{U}(0.2, 2.0)$ (Macquart et al. 2020). The GW population model parameters include α , β , m_{\min} , m_{\max} , Δm , μ_g , σ_g , λ_{peak} , γ , κ , and z_p , which are fixed to the inferred values of Abbott et al. (2023a).

We utilize the `bilby`³ package to perform Markov Chain Monte Carlo (MCMC) analysis and choose the `emcee`⁴ sampler. We use the `ICAROGW`⁵ package to do the hierachic Bayesian analysis of GW standard sirens, and the `GetDist`⁶ package to plot the marginalized posterior distributions. The final likelihood \mathcal{L} used in our analysis is the combination of \mathcal{L}_{FRB} and \mathcal{L}_{GW} in Eqs. (6) and (8), respectively, which is

Table 1. 1σ constraints on cosmological parameters Ω_b and H_0 .

Data	Ω_b	H_0
FRB	$0.0520^{+0.0120}_{-0.0280}$	$77.0^{+20.0}_{-40.0}$
FRB + GW	0.0488 ± 0.0064	$71.6^{+4.4}_{-8.6}$
FRB (TNG) + GW	0.0491 ± 0.0054	$71.2^{+4.4}_{-8.0}$
FRB (TNG + $f_d(z)$) + GW	$0.0510^{+0.0055}_{-0.0050}$	$71.8^{+4.5}_{-8.6}$
FRB + H_0 (Planck18 prior)	0.0513 ± 0.0046	67.4 ± 0.5
FRB + H_0 (SH0ES prior)	0.0473 ± 0.0043	73.0 ± 1.0

NOTE— The results are derived from 104 localized FRBs alone or in combination with 47 GW events, under different assumptions. For all cases, the 1σ constraints on DM parameters are $f_d = 0.90 \pm 0.04$, $F = 0.36^{+0.13}_{-0.05}$, $\mu_{\text{host}} = 4.67^{+0.20}_{-0.16}$, and $\sigma_{\text{host}} = 0.95^{+0.09}_{-0.13}$. H_0 is in units of $\text{km s}^{-1} \text{ Mpc}^{-1}$.

² This prior on f_d is informed by observations of the baryon fraction in stars (f_*) and cold gas (f_{cold}), independent of FRBs. Assuming a conservative flat prior for f_* extended by a factor of five, the diffuse baryon fraction is inferred via $f_d = 1 - f_* - f_{\text{cold}}$ (Connor et al. 2025).

³ <https://github.com/bilby-dev/bilby>

⁴ <https://emcee.readthedocs.io/en/stable>

⁵ <https://github.com/simone-mastrogiovanni/icarogw>

⁶ <https://github.com/cmbant/getdist>

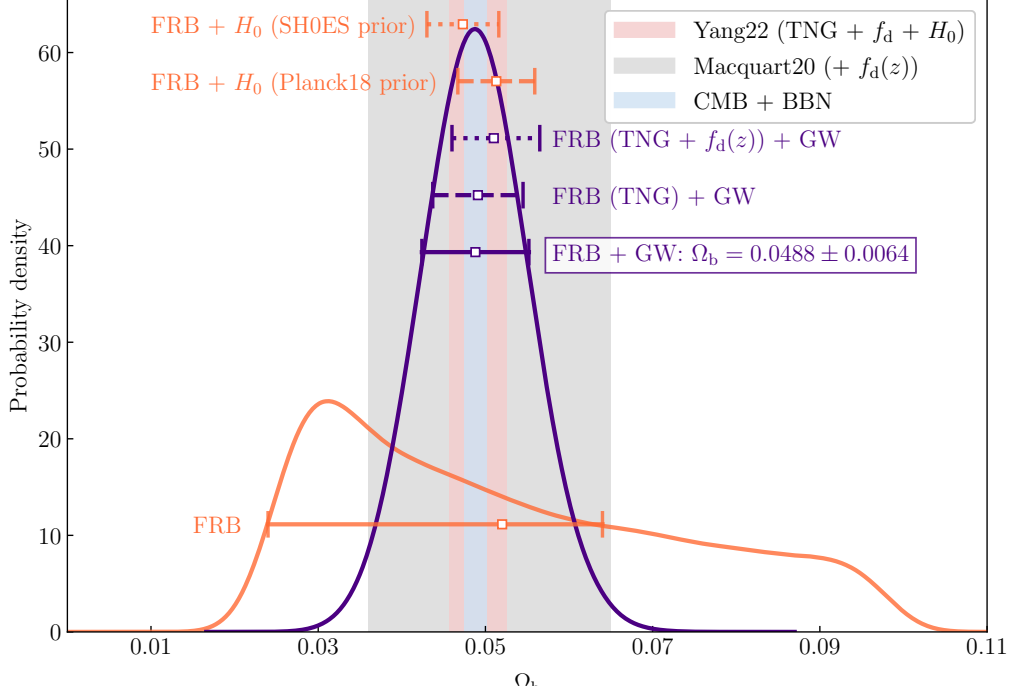


Figure 1. Normalized posterior distributions of Ω_b from 104 FRBs (orange) and 104 FRBs + 47 GWs (indigo). The median and 1σ credible interval from FRB + GW is $\Omega_b = 0.0488 \pm 0.0064$, marginalized over f_d and empirical DM model parameters. The errorbars in different colors and linestyles are shown under different assumptions: FRB + H_0 (Planck18 prior) and FRB + H_0 (SH0ES prior) adopt Gaussian priors on H_0 from Planck18 (Aghanim et al. 2020) and SH0ES (Riess et al. 2022), respectively; FRB (TNG) + GW and FRB (TNG + $f_d(z)$) + GW adopt priors on empirical DM model parameters from the IllustrisTNG simulation (Zhang et al. 2020, 2021) and on f_d from the redshift-dependent form of Macquart20 (Macquart et al. 2020), respectively. The blue, gray, and red shaded bands show the results from CMB + BBN (Cooke et al. 2018), Macquart20, and Yang22 (Yang et al. 2022), respectively. Note that Yang22 adopts the TNG prior, a flat prior on $H_0 \in \mathcal{U}(67, 73) \text{ km s}^{-1} \text{ Mpc}^{-1}$, and $f_d = 0.82$. All results are at the 1σ level.

written as

$$\ln \mathcal{L} = \ln (\mathcal{L}_{\text{FRB}}) + \ln (\mathcal{L}_{\text{GW}}). \quad (10)$$

3. RESULTS AND DISCUSSIONS

In this section, we report and discuss the constraints on Ω_b in Table 1. The posteriors for Ω_b and the corresponding credible intervals are shown in Figure 1. Using FRB data alone yields a relatively weak constraint of $\Omega_b = 0.052^{+0.012}_{-0.028}$ at the 1σ level. Incorporating GW standard sirens significantly narrows this to $\Omega_b = 0.0488 \pm 0.0064$, by breaking the strong degeneracy between Ω_b and H_0 via the independent H_0 measurement provided by GWs. Remarkably, this late-Universe estimate exhibits concordance with early-Universe values from BBN and CMB at the $\sim 13\%$ level, linking the gap between the early and late Universe. Note that a similarly precise constraint is simultaneously obtained for the Hubble constant, $H_0 = 71.6^{+4.4}_{-8.6} \text{ km s}^{-1} \text{ Mpc}^{-1}$, primarily driven by the GW dataset alone, which gives $H_0 = 72.6^{+5.2}_{-8.9} \text{ km s}^{-1} \text{ Mpc}^{-1}$. More data is required to arbitrate the H_0 tension. A detailed discussion on H_0 and DM parameters is provided in Appendix A.

We compare our Ω_b results with those from previous works. Macquart20 and Yang22 constrained Ω_b using differ-

ent samples of localized FRBs under external assumptions of $H_0 = 70 \text{ km s}^{-1} \text{ Mpc}^{-1}$ and a flat prior on $H_0 \in \mathcal{U}(67, 73) \text{ km s}^{-1} \text{ Mpc}^{-1}$, as shown by the gray and red bands in Figure 1, respectively. The constraint from Yang22 compares favorably to ours, since the current GW standard siren sample remains too limited to outperform their adopted H_0 prior. Applying the external H_0 priors from Planck18 or SH0ES to our FRB sample alone yields $\Omega_b = 0.0513 \pm 0.0046$ and $\Omega_b = 0.0473 \pm 0.0043$, respectively; the corresponding error bars are shown in Figure 1. This suggests that the H_0 tension would lead to two biased Ω_b estimates. Although the induced “ Ω_b inconsistency” in our sample is within 1σ uncertainty ($\sim 0.95\sigma$), it may become non-negligible with larger samples in updated DM analyses. Nevertheless, the joint FRB + GW result assumes no prior on H_0 and instead provides a late-Universe measurement of baryons, independent of both CMB and local distance ladder. This FRB + GW synergy may establish a novel paradigm for the cosmic baryon census, analogous to CMB + BBN, and serve as a powerful low-redshift cosmological probe in the era of next-generation FRB and GW surveys (Zhang et al. 2023).

We also investigate potential improvements to our results. FRB cosmology is subject to uncontrolled systematics mainly from modeling DM_{IGM} and DM_{host} distribu-

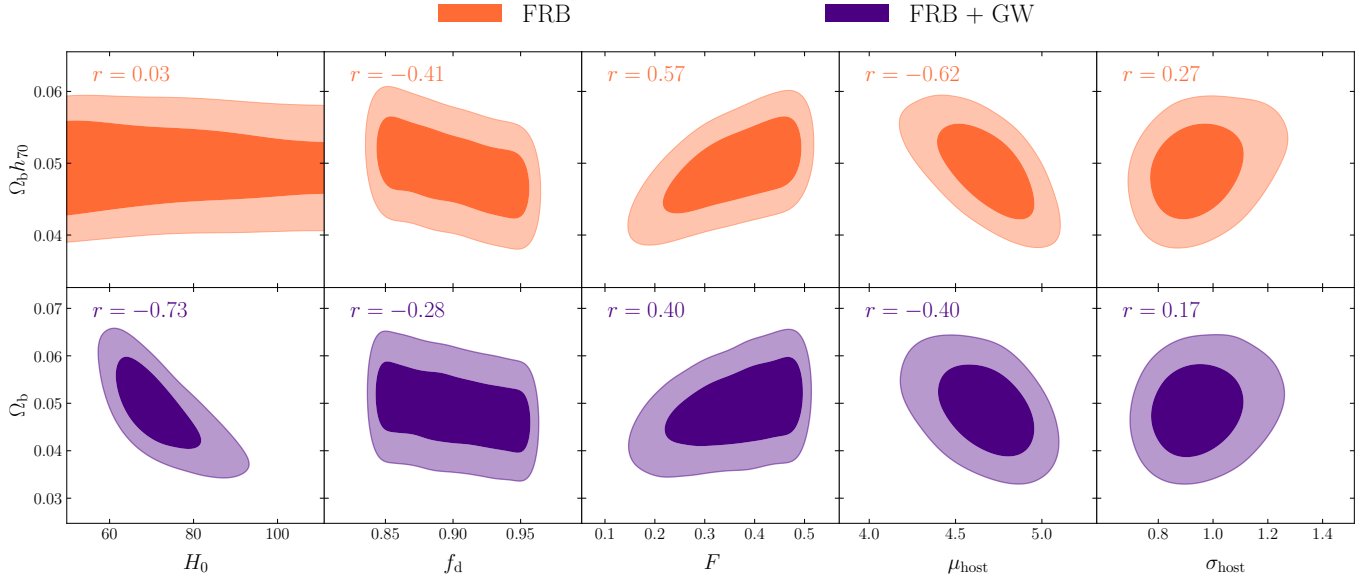


Figure 2. Posterior distributions (1σ and 2σ credible regions) for Ω_b and $\Omega_b h_{70}$ versus H_0 , f_d , F , μ_{host} , and σ_{host} , using FRB (orange) and FRB + GW (purple) data. The correlation coefficient r is labeled in each panel to quantify parameter degeneracies.

tions, as well as the weakly constrained f_d , which affects the mean value of DM_{IGM} . To reduce these systematics, cosmological simulations are commonly used to calibrate these DM parameters (F , μ_{host} , σ_{host} , and f_d) at different redshifts. Accordingly, we consider two cases with simulation-based priors: (i) fixing the empirical DM model parameters to the best-fit results from the IllustrisTNG simulation (hereafter TNG) (Zhang et al. 2020, 2021); and (ii) further fixing f_d to a redshift-dependent form following Macquart20, as implemented in the public FRB code⁷. The constraints from FRB (TNG) + GW and FRB (TNG + $f_d(z)$) + GW are $\Omega_b = 0.0491 \pm 0.0054$ and $\Omega_b = 0.0507 \pm 0.0052$, respectively, with the corresponding errorbars shown in Figure 1. Both results are consistent with the FRB + GW constraint within the 1σ uncertainty, suggesting that the simulation-based priors can improve current constraints without introducing significant bias. However, such agreement at the current level does not ensure the absence of systematic errors when applied to larger future FRB and GW samples, in which systematic errors may become dominant. Therefore, a detailed assessment of how the DM parameters affect the inferred baryon density is of great importance.

To assess the impact of systematic uncertainties on Ω_b and verify the robustness of our constraint, we analyze the parameter correlations using the FRB + GW dataset. The lower row of Figure 2 shows the marginalized posteriors of Ω_b and other relevant parameters, with correlation coefficients r labeled in each panel to quantify parameter degeneracies.

On the one hand, the degeneracy between Ω_b and H_0 is the strongest among all parameter pairs ($r = -0.73$), implying that the inferred value of Ω_b is highly sensitive to how H_0 is determined. While FRB + H_0 analyses rely on external priors, which are controversial due to the H_0 tension, FRB + GW analyses rely on GW data to provide H_0 , which is uniquely derived from self-calibrating absolute distance measurements. Therefore, the Ω_b constraint from FRB + GW is robust against the H_0 -related bias and free from assumptions affected by the H_0 tension.

On the other hand, the correlations between Ω_b and DM parameters are moderate. These DM parameters are not properly constrained, both in this work (see Appendix A for details) and earlier studies (James et al. 2022), and thus act as nuisance parameters that bias the inferred Ω_b . In the joint FRB + GW analysis, the correlation coefficients between Ω_b and f_d , F , μ_{host} , and σ_{host} are -0.28 , 0.40 , -0.40 , and 0.17 , respectively. For comparison, the upper row of Figure 2 shows the constraint on $\Omega_b h_{70}$, where $h_{70} = H_0 / (70 \text{ km s}^{-1} \text{ Mpc}^{-1})$. This parameter absorbs the strong degeneracy, enabling it to be effectively constrained using FRB data alone (Macquart et al. 2020; Connor et al. 2025). In this case, the corresponding correlations are notably stronger: -0.41 , 0.57 , -0.62 , and 0.27 , respectively. This comparison suggests that directly measuring Ω_b reduces degeneracies with the nuisance parameters and is more robust against the associated systematic uncertainties than $\Omega_b h_{70}$.

We conclude that incorporating GW data into the analysis of FRB dispersion measures enables a direct and effective measurement of Ω_b and, more importantly, avoids biases from the H_0 tension and mitigates those associated with nuisance model parameters. This demonstrates that the synergy

⁷ <https://github.com/FRBs/FRB>

between FRBs and GWs provides a robust estimate of the cosmic baryon density.

4. CONCLUSION

In this Letter, we combine two emerging cosmological probes, i.e., 104 localized FRBs and 47 GW standard sirens, to measure the cosmic baryon density in a robust manner. DM-based FRB cosmology struggles with various parameter degeneracies, particularly between H_0 and Ω_b . GWs can independently infer H_0 from self-calibrated luminosity distances obtained through waveform analysis as sirens, thus breaking the Ω_b - H_0 degeneracy. This joint analysis yields a constraint of $\Omega_b = 0.0488 \pm 0.0064$ (1σ), which is remarkably consistent with early-Universe values from BBN and CMB at the $\sim 13\%$ level and provides a purely late-Universe perspective on resolving the missing baryon problem. We also obtain a simultaneous constraint on the Hubble constant, $H_0 = 71.6^{+4.4}_{-8.6} \text{ km s}^{-1} \text{ Mpc}^{-1}$, primarily driven by the GW data. Together, these results exhibit Ω_b - H_0 concordance between the early and late Universe.

Moreover, we explore two prior-based scenarios: (i) H_0 -prior-based cases using FRB data alone, where adopting Gaussian priors from Planck18 and SH0ES yields $\Omega_b = 0.0513 \pm 0.0046$ and $\Omega_b = 0.0473 \pm 0.0043$, respectively. These results indicate that the H_0 tension would bias baryon density estimates, although the induced “ Ω_b inconsistency” remains within 1σ uncertainty in our sample. (ii) Simulation-based prior cases using FRB + GW, where fixing empirical DM model parameters from the IllustrisTNG simulation and further fixing f_d to a redshift-dependent form yield $\Omega_b = 0.0491 \pm 0.0054$ and 0.0507 ± 0.0052 , respectively. These two results agree with that of FRB + GW at the 1σ level, indicating that simulation-based priors can improve current constraints without introducing significant bias. However, in both (i) and (ii), systematic effects from external assumptions (related to H_0 , f_d , and empirical DM model parameters) may

become non-negligible when applied to larger future FRB and GW samples.

Hence, we assess the associated systematic uncertainties through a detailed correlation analysis. On the one hand, the dominant uncertainty is the degeneracy between Ω_b and H_0 , implying the importance of carefully addressing the H_0 -related bias. Unlike prior-based analyses that rely on assumed values of H_0 , the joint FRB + GW analysis avoids such bias by uniquely inferring H_0 from the absolute distances provided by GWs, independent of both CMB and local distance ladder. On the other hand, the correlations between Ω_b and DM parameters—treated as nuisance parameters—are moderate, and notably weaker than those of $\Omega_b h_{70}$, making the direct inference of Ω_b more robust against the uncertainties induced by the nuisance parameters. Therefore, combining FRB and GW data not only avoids the bias induced by the H_0 tension, but also mitigates model-dependent uncertainties.

Overall, the novel combination of FRBs and GWs enables a direct, unique, and robust measurement of both the baryon content and cosmological distances at low redshifts. With an increasing number of GW detections expected in the upcoming LVK run, and potentially thousands of localized FRBs expected from CHIME/Outriggers (Masui 2023) and DSA-110 (Law et al. 2024), their synergy will soon emerge as a powerful low-redshift cosmological probe.

5. ACKNOWLEDGMENTS

We thank Tian-Nuo Li, Meng-Lin Zhao, Yang Liu, and Qin Wu for fruitful discussions. This work was supported by the National SKA Program of China (grant Nos. 2022SKA0110200 and 2022SKA0110203), the National Natural Science Foundation of China (grant Nos. 12473001, 11975072, 11875102, and 11835009), the China Manned Space Program (grant No. CMS-CSST-2025-A02), and the National 111 Project (grant No. B16009).

APPENDIX

A. CONSTRAINTS ON H_0 AND DM PARAMETERS

In this Appendix, we report and discuss the constraints on H_0 and DM parameters (f_d , F , μ_{host} , and σ_{host}).

The constraints on H_0 are listed in Table 1, and posteriors and corresponding credible intervals for H_0 are shown in Figure 3. A direct measurement of H_0 using FRBs alone is difficult due to strong parameter degeneracies. Specifically, our measurement using FRBs alone is $H_0 = 77.0^{+20.0}_{-40.0} \text{ km s}^{-1} \text{ Mpc}^{-1}$, and the inclusion of GW data narrows the constraint to $H_0 = 71.6^{+4.4}_{-8.6} \text{ km s}^{-1} \text{ Mpc}^{-1}$. This improvement is mainly driven by the GW data itself, which yields $H_0 = 72.6^{+5.2}_{-8.9} \text{ km s}^{-1} \text{ Mpc}^{-1}$. Previous studies predominantly inferred H_0 by fixing the baryon density parameter at the early-Universe value. For example, Wu et al. (2022) (hereafter Wu22) and James et al. (2022) (hereafter James22) used different FRB samples to derive $H_0 = 69.31^{+6.21}_{-6.63} \text{ km s}^{-1} \text{ Mpc}^{-1}$ and $H_0 = 73^{+12}_{-8} \text{ km s}^{-1} \text{ Mpc}^{-1}$, by assuming external priors on $\Omega_b h^2 \sim \mathcal{N}(0.02235, 0.00049)$ from BBN and $\Omega_b h^2 = 0.02242$ from Planck18, respectively, which are shown as red and gray bands in Figure 3. Recently, Wang et al. (2025) and Gao et al. (2025a) also used 92 and 108 localized FRBs to obtain $H_0 = 69.04^{+2.30}_{-2.07} \text{ km s}^{-1} \text{ Mpc}^{-1}$ and $H_0 = 69.40^{+2.14}_{-1.97} \text{ km s}^{-1} \text{ Mpc}^{-1}$, respectively, both assuming BBN and TNG priors. Using the same BBN prior, we obtain

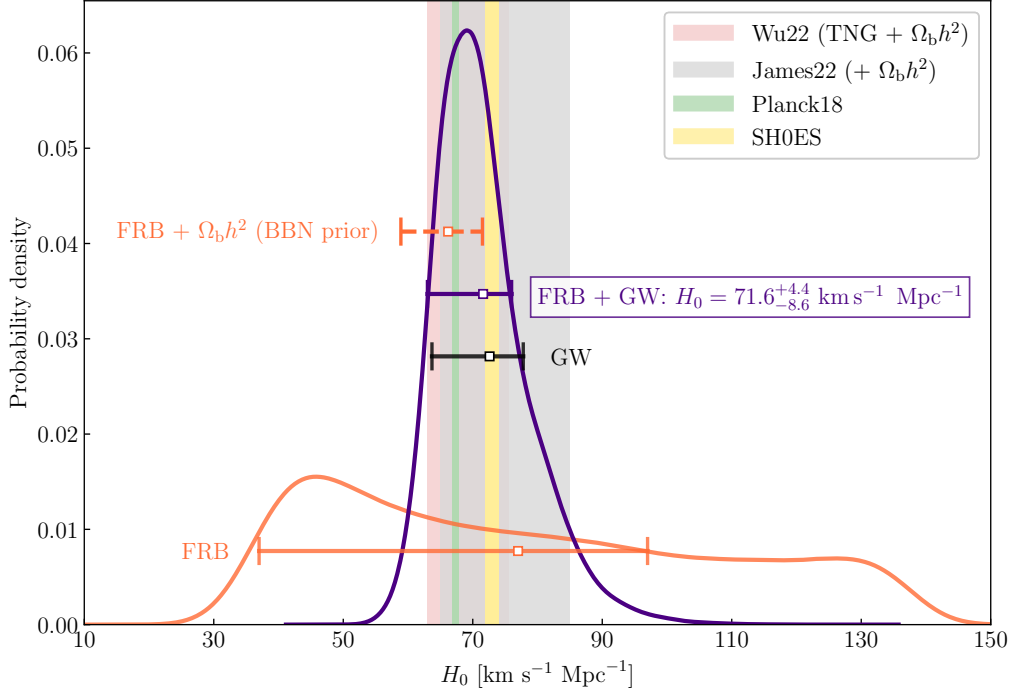


Figure 3. Same as Figure 1 but for posterior distribution of H_0 . The median and 1σ credible interval from FRB + GW is $H_0 = 71.6^{+4.4}_{-8.6} \text{ km s}^{-1} \text{ Mpc}^{-1}$. The orange and black errorbars correspond to constraints from FRB + $\Omega_b h^2$ (BBN prior (Cooke et al. 2018)) and GW data alone, respectively. The green, yellow, red, and gray shaded bands denote the results from Planck18 (Aghanim et al. 2020), SH0ES (Riess et al. 2022), Wu22 (Wu et al. 2022), and James22 (James et al. 2022), respectively. Note that Wu22 adopts the TNG prior, and both Wu22 and James22 adopt $\Omega_b h^2$ priors from BBN (Cooke et al. 2018) and CMB (Aghanim et al. 2020), respectively. All results are at 1σ uncertainty.

$H_0 = 66.2^{+5.3}_{-7.3} \text{ km s}^{-1} \text{ Mpc}^{-1}$ from FRB + $\Omega_b h^2$, which slightly favors the Planck18 result with a precision comparable to that of FRB + GW. Unlike prior-based methods, the FRB + GW constraint provides a late-Universe result of H_0 . More data is required to offer further insight into arbitrating the H_0 tension. Notably, time-delay cosmography using strongly lensed FRBs by massive galaxies can offer an independent measurement of H_0 , since the time delays between lensed FRB images can be determined with exceptional precision (Li et al. 2018; Zhang et al. 2025a).

For DM parameters, the constraints are $f_d = 0.90 \pm 0.04$, $F = 0.36^{+0.13}_{-0.05}$, $\mu_{\text{host}} = 4.67^{+0.20}_{-0.16}$, and $\sigma_{\text{host}} = 0.95^{+0.09}_{-0.13}$. The inclusion of GW data has a negligible impact on this constraint. For the host contribution, the results of μ_{host} and σ_{host} correspond to a median rest-frame host DM of $108 \pm 20 \text{ pc cm}^{-3}$ (corresponding mean DM is $168^{+57}_{-40} \text{ pc cm}^{-3}$), which is consistent with both $\text{DM}_{\text{host}} = 103^{+68}_{-48} \text{ pc cm}^{-3}$ (Yang et al. 2025) and $\text{DM}_{\text{host}} = 130^{+25}_{-23} \text{ pc cm}^{-3}$ (Connor et al. 2025).

B. FRB DATA

In this Appendix, we list the properties of the 104 localized FRBs used in this work in Table 2.

Table 2. Properties of 104 localized FRBs.

Name	Redshift	DM _{obs}	DM _{MW,ISM} (NE2001)	R.A. (J2000)	Decl. (J2000)	Host Type	Reference
		(pc cm ⁻³)	(pc cm ⁻³)	(°)	(°)		
FRB 20121102A	0.19273	557	188.4	82.9946	33.1479	1	Chatterjee et al. (2017) Tendulkar et al. (2017)
FRB 20180301A	0.3304	552	151.7	93.2268	4.6711	1	Bhandari et al. (2022)
FRB 20180924B	0.3214	361.42	40.5	326.1053	-40.9	3	Bannister et al. (2019)

Table 2 continued

Table 2 (continued)

Name	Redshift	DM _{obs}	DM _{MW,ISM} (NE2001)	R.A. (J2000)	Decl. (J2000)	Host Type	Reference
		(pc cm ⁻³)	(pc cm ⁻³)	($^{\circ}$)	($^{\circ}$)		
FRB 20181112A	0.4755	589.27	41.7	327.3485	-52.9709	3	Prochaska et al. (2019)
FRB 20181223C	0.03024	111.61	19.9	180.9207	27.5476	3	Bhardwaj et al. (2024)
FRB 20190102C	0.2912	364.5	57.4	322.4157	-79.4757	3	Bhandari et al. (2020)
FRB 20190110C	0.12244	221.6	37.1	249.3185	41.4434	2	Ibik et al. (2024)
FRB 20190303A	0.064	223.2	29.8	207.9958	48.1211	2	Michilli et al. (2023)
FRB 20190418A	0.07132	182.78	70.2	65.8123	16.0738	3	Bhardwaj et al. (2024)
FRB 20190523A	0.66	760.8	37.2	207.065	72.4697	3	Ravi et al. (2019)
FRB 20190608B	0.11778	338.7	37.3	334.0199	-7.8983	3	Chittidi et al. (2021)
FRB 20190611B	0.3778	321.4	57.8	320.7456	-79.3976	3	Heintz et al. (2020)
FRB 20190614D	0.6	959.2	87.8	65.0755	73.7067	3	Law et al. (2020)
FRB 20190711A	0.522	593.1	56.5	329.4193	-80.358	1	Heintz et al. (2020)
FRB 20190714A	0.2365	504.13	38.5	183.9797	-13.021	3	Heintz et al. (2020)
FRB 20191001A	0.234	506.92	44.2	323.3513	-54.7478	3	Heintz et al. (2020)
FRB 20191106C	0.10775	332.2	25	199.5801	42.9997	2	Ibik et al. (2024)
FRB 20191228A	0.2432	297.5	32.9	344.4304	-28.5941	3	Bhandari et al. (2022)
FRB 20200223B	0.06024	201.8	45.6	8.2695	28.8313	2	Ibik et al. (2024)
FRB 20200430A	0.1608	380.1	27.2	229.7064	12.3763	3	Heintz et al. (2020)
FRB 20200723B	0.0085	244	33	190.1583	-5.135	3	Shin et al. (2024)
FRB 20200906A	0.3688	577.8	35.8	53.4962	-14.0832	3	Bhandari et al. (2022)
FRB 20201124A	0.098	413.52	139.9	77.0146	26.0607	2	Ravi et al. (2022)
FRB 20210117A	0.2145	729.1	34.4	339.9792	-16.1515	3	Bhandari et al. (2023)
FRB 20210320C	0.2797	384.8	39.3	204.4608	-16.1227	3	Shannon et al. (2025)
FRB 20210410D	0.1415	571.2	56.2	326.0863	-79.3182	3	Caleb et al. (2023)
FRB 20210603A	0.1772	500.147	39.5	10.2741	21.2263	3	Cassanelli et al. (2024)
FRB 20210807D	0.1293	251.3	121.2	299.2214	-0.7624	3	Gordon et al. (2023)
FRB 20211127I	0.0469	234.83	42.5	199.8082	-18.8378	3	Gordon et al. (2023)
FRB 20211203C	0.3439	636.2	63.7	204.5625	-31.3801	3	Gordon et al. (2023)
FRB 20211212A	0.0715	206	27.1	157.3509	1.676889	3	Gordon et al. (2023)
FRB 20220105A	0.2785	583	22	208.8039	22.4665	3	Gordon et al. (2023)
FRB 20220204A	0.4012	612.584	50.7	274.2263	69.7225	3	Sharma et al. (2024)
FRB 20220207C	0.04304	262.38	76.1	310.1995	72.8823	3	Law et al. (2024)
FRB 20220208A	0.351	437	101.6	319.3483	71.54	3	Sharma et al. (2024)
FRB 20220307B	0.2507	499.15	128.2	350.8745	72.1924	3	Law et al. (2024)
FRB 20220310F	0.477958	462.24	46.3	134.7204	73.4908	3	Law et al. (2024)
FRB 20220330D	0.3714	468.1	38.6	165.7256	71.7535	3	Sharma et al. (2024)
FRB 20220418A	0.622	623.25	36.7	219.1056	70.0959	3	Law et al. (2024)
FRB 20220501C	0.381	449.5	30.6	352.3792	-32.4907	3	Shannon et al. (2025)
FRB 20220506D	0.30039	396.97	84.6	318.0448	72.8273	3	Law et al. (2024)
FRB 20220509G	0.0894	269.53	55.6	282.67	70.2438	3	Law et al. (2024)
FRB 20220521B	1.354	1342.9	138.8	351.036	71.138	3	Shannon et al. (2025)
FRB 20220529A	0.1839	246	40	19.1042	20.6325	1	Li et al. (2025)
FRB 20220610A	1.016	1458.15	31	351.0732	-33.5137	3	Ryder et al. (2023)
FRB 20220717A	0.36295	637.34	118.3	293.3042	-19.2877	3	Rajwade et al. (2024)
FRB 20220725A	0.1926	290.4	30.7	353.3152	-35.9902	3	Shannon et al. (2025)
FRB 20220726A	0.361	686.55	89.5	73.94567	69.9291	3	Sharma et al. (2024)
FRB 20220825A	0.241397	651.24	78.5	311.9815	72.585	3	Law et al. (2024)
FRB 20220914A	0.1139	631.28	54.7	282.0568	73.3369	3	Law et al. (2024)
FRB 20220918A	0.491	656.8	153.1	17.5921	70.8113	3	Shannon et al. (2025)
FRB 20220920A	0.158239	314.99	39.9	240.2571	70.9188	3	Law et al. (2024)
FRB 20221012A	0.284669	441.08	54.3	280.7987	70.5242	3	Law et al. (2024)
FRB 20221027A	0.229	452.5	47.2	129.6104	71.7315	3	Sharma et al. (2024)
FRB 20221029A	0.975	1391.75	43.8	141.9634	72.4523	3	Sharma et al. (2024)

Table 2 continued

Table 2 (continued)

Name	Redshift	DM _{obs}	DM _{MW,ISM} (NE2001)	R.A. (J2000)	Decl. (J2000)	Host Type	Reference
		(pc cm ⁻³)	(pc cm ⁻³)	($^{\circ}$)	($^{\circ}$)		
FRB 20221101B	0.2395	491.554	131.2	342.2162	70.6812	3	Sharma et al. (2024)
FRB 20221106A	0.2044	343.8	34.8	56.7048	-25.5698	3	Shannon et al. (2025)
FRB 20221113A	0.2505	411.027	91.7	71.411	70.3074	3	Sharma et al. (2024)
FRB 20221116A	0.2764	643.448	132.3	21.2102	72.6539	3	Sharma et al. (2024)
FRB 20221219A	0.553	706.708	44.4	257.6298	71.6268	3	Sharma et al. (2024)
FRB 20230124A	0.0939	590.574	38.6	231.9163	70.9681	3	Sharma et al. (2024)
FRB 20230203A	0.1464	420.1	67.299	151.66159	35.6941	3	Amiri et al. (2025)
FRB 20230216A	0.531	828	38.5	155.9717	1.4678	3	Sharma et al. (2024)
FRB 20230222A	0.1223	706.1	33.31	106.96036	11.22452	3	Amiri et al. (2025)
FRB 20230222B	0.11	187.8	56.9977	238.73912	30.8987	3	Amiri et al. (2025)
FRB 20230307A	0.271	608.9	37.6	177.7813	71.6956	3	Sharma et al. (2024)
FRB 20230311A	0.1918	364.3	67.2352	91.10966	55.94595	3	Amiri et al. (2025)
FRB 20230501A	0.301	532.5	125.6	340.0272	70.9222	3	Sharma et al. (2024)
FRB 20230506C	0.3896	772	68	12.0998	42.0061	2	Anna-Thomas et al. (2025)
FRB 20230526A	0.157	361.4	31.9	22.2326	-52.7173	3	Shannon et al. (2025)
FRB 20230626A	0.327	451.2	39.2	240.7125	71.7142	3	Sharma et al. (2024)
FRB 20230628A	0.1265	344.952	39	166.7867	72.2818	3	Sharma et al. (2024)
FRB 20230703A	0.1184	291.3	38.1566	184.62445	48.72993	3	Amiri et al. (2025)
FRB 20230708A	0.105	411.51	60.3	303.1155	-55.3563	3	Shannon et al. (2025)
FRB 20230712A	0.4525	587.567	39.2	167.3585	72.5578	3	Sharma et al. (2024)
FRB 20230730A	0.2115	312.5	114.6465	54.66456	33.1593	3	Amiri et al. (2025)
FRB 20230808F	0.3472	653.2	31	53.3041	-51.9353	3	Hanmer et al. (2025)
FRB 20230814A	0.553	696.4	104.8	335.9748	73.0259	3	Connor et al. (2025)
FRB 20230902A	0.3619	440.1	34.1	52.1398	-47.3335	3	Shannon et al. (2025)
FRB 20230930A	0.0925	456	70	10.5	41.4	3	Anna-Thomas et al. (2025)
FRB 20231011A	0.0783	186.3	58.5524	18.2411	41.7491	3	Amiri et al. (2025)
FRB 20231017A	0.245	344.2	31.1515	346.75429	36.65268	3	Amiri et al. (2025)
FRB 20231025B	0.3238	368.7	65.5787	270.78807	63.98908	3	Amiri et al. (2025)
FRB 20231120A	0.07	438.9	43.8	143.6169	71.7574	3	Sharma et al. (2024)
FRB 20231123A	0.0729	302.1	37.1085	82.62325	4.47554	3	Amiri et al. (2025)
FRB 20231123B	0.2625	396.7	40.2	242.5382	70.7851	3	Sharma et al. (2024)
FRB 20231128A	0.1079	331.6	64.7368	199.5782	42.99271	1	Amiri et al. (2025)
FRB 20231204A	0.0644	221	34.9372	207.99903	48.116	2	Amiri et al. (2025)
FRB 20231206A	0.0659	457.7	37.5114	112.44284	56.25627	3	Amiri et al. (2025)
FRB 20231220A	0.3355	491.2	49.9	123.9087	73.6599	3	Connor et al. (2025)
FRB 20231226A	0.1569	329.9	38.1	155.3638	6.1103	3	Shannon et al. (2025)
FRB 20231229A	0.019	198.5	65.1335	26.46783	35.11292	3	Amiri et al. (2025)
FRB 20231230A	0.0298	131.4	32.2305	72.79761	2.39398	3	Amiri et al. (2025)
FRB 20240114A	0.13	527.65	49.7	321.9161	4.3292	1	Tian et al. (2024)
FRB 20240119A	0.376	483.1	38	224.4672	71.6118	3	Connor et al. (2025)
FRB 20240123A	0.968	1462	90.2	68.2625	71.9453	3	Connor et al. (2025)
FRB 20240201A	0.042729	374.5	38.6	149.9056	14.088	3	Shannon et al. (2025)
FRB 20240209A	0.1384	176.518	63.1	289.8504	86.0609	2	Eftekhari et al. (2025)
FRB 20240210A	0.023686	283.73	28.7	8.7796	-28.2708	3	Shannon et al. (2025)
FRB 20240213A	0.1185	357.4	40	166.1683	74.0754	3	Connor et al. (2025)
FRB 20240215A	0.21	549.5	47.9	268.4413	70.2324	3	Connor et al. (2025)
FRB 20240229A	0.287	491.15	38	169.9835	70.6762	3	Connor et al. (2025)
FRB 20240304A	0.2423	652.6	73.9	136.3304	-16.2282	3	Shannon et al. (2025)
FRB 20240310A	0.127	601.8	30.1	17.6219	-44.4394	3	Shannon et al. (2025)

NOTE— The listed properties include redshift, right ascension (R.A.), declination (Decl.), observed dispersion measure (DM), the Milky Way ISM contribution derived from the NE2001 model, and types of their host galaxies. The host types are classified into three categories: type 1 refers to repeating FRBs in dwarf galaxies, type 2 to repeating FRBs in spiral galaxies, and type 3 to one-off FRBs.

REFERENCES

- Abbott, B. P., et al. 2017a, *Nature*, 551, 85, doi: [10.1038/nature24471](https://doi.org/10.1038/nature24471)
- . 2017b, *Phys. Rev. Lett.*, 119, 161101, doi: [10.1103/PhysRevLett.119.161101](https://doi.org/10.1103/PhysRevLett.119.161101)
- Abbott, B. P., Abbott, R., Abbott, T. D., et al. 2017c, *The Astrophysical Journal Letters*, 848, L13, doi: [10.3847/2041-8213/aa920c](https://doi.org/10.3847/2041-8213/aa920c)
- Abbott, R., et al. 2023a, *Astrophys. J.*, 949, 76, doi: [10.3847/1538-4357/ac74bb](https://doi.org/10.3847/1538-4357/ac74bb)
- Abbott, R., Abbott, T., Acernese, F., et al. 2023b, *Physical Review X*, 13, doi: [10.1103/physrevx.13.011048](https://doi.org/10.1103/physrevx.13.011048)
- Abdalla, E., et al. 2022, *JHEAp*, 34, 49, doi: [10.1016/j.jheap.2022.04.002](https://doi.org/10.1016/j.jheap.2022.04.002)
- Aghanim, N., Akrami, Y., Ashdown, M., et al. 2020, *Astronomy & Astrophysics*, 641, A6, doi: [10.1051/0004-6361/201833910](https://doi.org/10.1051/0004-6361/201833910)
- Amiri, M., et al. 2025. <https://arxiv.org/abs/2502.11217>
- Anna-Thomas, R., Law, C. J., Koch, E. W., et al. 2025, arXiv e-prints, arXiv:2503.02947, doi: [10.48550/arXiv.2503.02947](https://doi.org/10.48550/arXiv.2503.02947)
- Bannister, K. W., Deller, A. T., Phillips, C., et al. 2019, *Science*, 365, 565, doi: [10.1126/science.aaw5903](https://doi.org/10.1126/science.aaw5903)
- Bhandari, S., & Flynn, C. 2021, *Universe*, 7, 85, doi: [10.3390/universe7040085](https://doi.org/10.3390/universe7040085)
- Bhandari, S., Sadler, E. M., Prochaska, J. X., et al. 2020, *ApJL*, 895, L37, doi: [10.3847/2041-8213/ab672e](https://doi.org/10.3847/2041-8213/ab672e)
- Bhandari, S., Heintz, K. E., Aggarwal, K., et al. 2022, *AJ*, 163, 69, doi: [10.3847/1538-3881/ac3aec](https://doi.org/10.3847/1538-3881/ac3aec)
- Bhandari, S., Gordon, A. C., Scott, D. R., et al. 2023, *ApJ*, 948, 67, doi: [10.3847/1538-4357/acc178](https://doi.org/10.3847/1538-4357/acc178)
- Bhardwaj, M., Michilli, D., Kirichenko, A. Y., et al. 2024, *ApJ*, 971, L51, doi: [10.3847/2041-8213/ad64d1](https://doi.org/10.3847/2041-8213/ad64d1)
- Cai, R.-G., Liu, T.-B., Liu, X.-W., Wang, S.-J., & Yang, T. 2018, *Phys. Rev. D*, 97, 103005, doi: [10.1103/PhysRevD.97.103005](https://doi.org/10.1103/PhysRevD.97.103005)
- Cai, R.-G., & Yang, T. 2017, *Phys. Rev. D*, 95, 044024, doi: [10.1103/PhysRevD.95.044024](https://doi.org/10.1103/PhysRevD.95.044024)
- Caleb, M., Driessen, L. N., Gordon, A. C., et al. 2023, *MNRAS*, 524, 2064, doi: [10.1093/mnras/stad1839](https://doi.org/10.1093/mnras/stad1839)
- Cassanelli, T., Leung, C., Sanghavi, P., et al. 2024, *Nat Astron.*, 8, 1429, doi: [10.1038/s41550-024-02357-x](https://doi.org/10.1038/s41550-024-02357-x)
- Cen, R., & Ostriker, J. P. 1999, *The Astrophysical Journal*, 514, 1
- Chatterjee, S., et al. 2017, *Nature*, 541, 58, doi: [10.1038/nature20797](https://doi.org/10.1038/nature20797)
- Chen, H.-Y., Fishbach, M., & Holz, D. E. 2018, *Nature*, 562, 545, doi: [10.1038/s41586-018-0606-0](https://doi.org/10.1038/s41586-018-0606-0)
- Chittidi, J. S., Simha, S., Mannings, A., et al. 2021, *ApJ*, 922, 173, doi: [10.3847/1538-4357/ac2818](https://doi.org/10.3847/1538-4357/ac2818)
- Connor, L., Ravi, V., Sharma, K., et al. 2025, *Nature Astronomy*, doi: [10.1038/s41550-025-02566-y](https://doi.org/10.1038/s41550-025-02566-y)
- Cooke, R. J., Pettini, M., & Steidel, C. C. 2018, *Astrophys. J.*, 855, 102, doi: [10.3847/1538-4357/aaab53](https://doi.org/10.3847/1538-4357/aaab53)
- Cordes, J. M., & Lazio, T. J. W. 2002, <https://arxiv.org/abs/astro-ph/0207156>
- Cutler, C., & Holz, D. E. 2009, *Phys. Rev. D*, 80, 104009, doi: [10.1103/PhysRevD.80.104009](https://doi.org/10.1103/PhysRevD.80.104009)
- Dalal, N., Holz, D. E., Hughes, S. A., & Jain, B. 2006, *Phys. Rev. D*, 74, 063006, doi: [10.1103/PhysRevD.74.063006](https://doi.org/10.1103/PhysRevD.74.063006)
- Dálya, G., et al. 2022, *Mon. Not. Roy. Astron. Soc.*, 514, 1403, doi: [10.1093/mnras/stac1443](https://doi.org/10.1093/mnras/stac1443)
- Deng, W., & Zhang, B. 2014, *Astrophys. J. Lett.*, 783, L35, doi: [10.1088/2041-8205/783/2/L35](https://doi.org/10.1088/2041-8205/783/2/L35)
- Di Valentino, E., Mena, O., Pan, S., et al. 2021, *Class. Quant. Grav.*, 38, 153001, doi: [10.1088/1361-6382/ac086d](https://doi.org/10.1088/1361-6382/ac086d)
- Dong, Y.-Y., Song, J.-Y., Jin, S.-J., Zhang, J.-F., & Zhang, X. 2024, <https://arxiv.org/abs/2404.18188>
- Eftekhari, T., Dong, Y., Fong, W., et al. 2025, *ApJL*, 979, L22, doi: [10.3847/2041-8213/ad9de2](https://doi.org/10.3847/2041-8213/ad9de2)
- Ezquiaga, J. M., & Holz, D. E. 2022, *Phys. Rev. Lett.*, 129, 061102, doi: [10.1103/PhysRevLett.129.061102](https://doi.org/10.1103/PhysRevLett.129.061102)
- Feng, L., Han, T., Zhang, J.-F., & Zhang, X. 2024, *Chin. Phys. C*, 48, 095104, doi: [10.1088/1674-1137/ad5ae4](https://doi.org/10.1088/1674-1137/ad5ae4)
- Fukugita, M., Hogan, C. J., & Peebles, P. J. E. 1998, *Astrophys. J.*, 503, 518, doi: [10.1086/306025](https://doi.org/10.1086/306025)
- Gao, D. H., Wu, Q., Hu, J. P., et al. 2025a, *Astron. Astrophys.*, 698, A215, doi: [10.1051/0004-6361/202453006](https://doi.org/10.1051/0004-6361/202453006)
- Gao, H., Li, Z., & Zhang, B. 2014, *Astrophys. J.*, 788, 189, doi: [10.1088/0004-637X/788/2/189](https://doi.org/10.1088/0004-637X/788/2/189)
- Gao, J., Zhou, Z., Du, M., et al. 2023, *Monthly Notices of the Royal Astronomical Society*, 527, 7861, doi: [10.1093/mnras/stad3708](https://doi.org/10.1093/mnras/stad3708)
- Gao, R., Gao, H., Li, Z., & Yang, Y.-P. 2025b, <https://arxiv.org/abs/2504.15119>
- Glowacki, M., & Lee, K.-G. 2025, *Reference Module in Materials Science and Materials Engineering*, doi: <https://doi.org/10.1016/B978-0-443-21439-4.00073-0>
- Gordon, A. C., Fong, W.-f., Kilpatrick, C. D., et al. 2023, *ApJ*, 954, 80, doi: [10.3847/1538-4357/ace5aa](https://doi.org/10.3847/1538-4357/ace5aa)
- Gray, R., et al. 2020, *Phys. Rev. D*, 101, 122001, doi: [10.1103/PhysRevD.101.122001](https://doi.org/10.1103/PhysRevD.101.122001)
- Gray, R., Beirnaert, F., Karathanasis, C., et al. 2023, *JCAP*, 12, 023, doi: [10.1088/1475-7516/2023/12/023](https://doi.org/10.1088/1475-7516/2023/12/023)
- Guo, R.-Y., Zhang, J.-F., & Zhang, X. 2019, *JCAP*, 02, 054, doi: [10.1088/1475-7516/2019/02/054](https://doi.org/10.1088/1475-7516/2019/02/054)
- Hagstotz, S., Reischke, R., & Lilow, R. 2022, *Mon. Not. Roy. Astron. Soc.*, 511, 662, doi: [10.1093/mnras/stac077](https://doi.org/10.1093/mnras/stac077)
- Han, T., Jin, S.-J., Zhang, J.-F., & Zhang, X. 2024, *Eur. Phys. J. C*, 84, 663, doi: [10.1140/epjc/s10052-024-12999-w](https://doi.org/10.1140/epjc/s10052-024-12999-w)
- Han, T., Zhang, J.-F., & Zhang, X. 2025, <https://arxiv.org/abs/2504.17741>

- Hanmer, K. Y., Pastor-Marazuela, I., Brink, J., et al. 2025, MNRAS, 538, 1800, doi: [10.1093/mnras/staf289](https://doi.org/10.1093/mnras/staf289)
- Heintz, K. E., Prochaska, J. X., Simha, S., et al. 2020, ApJ, 903, 152, doi: [10.3847/1538-4357/abb6fb](https://doi.org/10.3847/1538-4357/abb6fb)
- Hu, J.-P., & Wang, F.-Y. 2023, Universe, 9, 94, doi: [10.3390/universe9020094](https://doi.org/10.3390/universe9020094)
- Ibik, A. L., Drout, M. R., Gaensler, B. M., et al. 2024, ApJ, 961, 99, doi: [10.3847/1538-4357/ad0893](https://doi.org/10.3847/1538-4357/ad0893)
- James, C. W., et al. 2022, Mon. Not. Roy. Astron. Soc., 516, 4862, doi: [10.1093/mnras/stac2524](https://doi.org/10.1093/mnras/stac2524)
- Jaroszynski, M. 2019, Mon. Not. Roy. Astron. Soc., 484, 1637, doi: [10.1093/mnras/sty3529](https://doi.org/10.1093/mnras/sty3529)
- Jin, S.-J., He, D.-Z., Xu, Y., Zhang, J.-F., & Zhang, X. 2020, JCAP, 03, 051, doi: [10.1088/1475-7516/2020/03/051](https://doi.org/10.1088/1475-7516/2020/03/051)
- Jin, S.-J., Zhang, Y.-Z., Song, J.-Y., Zhang, J.-F., & Zhang, X. 2024a, Sci. China Phys. Mech. Astron., 67, 220412, doi: [10.1007/s11433-023-2276-1](https://doi.org/10.1007/s11433-023-2276-1)
- Jin, S.-J., Zhu, R.-Q., Song, J.-Y., et al. 2024b, JCAP, 08, 050, doi: [10.1088/1475-7516/2024/08/050](https://doi.org/10.1088/1475-7516/2024/08/050)
- Kochanek, C. S., Pahre, M. A., Falco, E. E., et al. 2001, Astrophys. J., 560, 566, doi: [10.1086/322488](https://doi.org/10.1086/322488)
- Kumar, P., & Linder, E. V. 2019, Phys. Rev. D, 100, 083533, doi: [10.1103/PhysRevD.100.083533](https://doi.org/10.1103/PhysRevD.100.083533)
- Law, C. J., Butler, B. J., Prochaska, J. X., et al. 2020, ApJ, 899, 161, doi: [10.3847/1538-4357/aba4ac](https://doi.org/10.3847/1538-4357/aba4ac)
- Law, C. J., et al. 2024, Astrophys. J., 967, 29, doi: [10.3847/1538-4357/ad3736](https://doi.org/10.3847/1538-4357/ad3736)
- Law, C. J., Sharma, K., Ravi, V., et al. 2024, ApJ, 967, 29, doi: [10.3847/1538-4357/ad3736](https://doi.org/10.3847/1538-4357/ad3736)
- Li, T.-N., Jin, S.-J., Li, H.-L., Zhang, J.-F., & Zhang, X. 2024, Astrophys. J., 963, 52, doi: [10.3847/1538-4357/ad1bc9](https://doi.org/10.3847/1538-4357/ad1bc9)
- Li, Y., et al. 2025. <https://arxiv.org/abs/2503.04727>
- Li, Z., Gao, H., Wei, J.-J., et al. 2020, Mon. Not. Roy. Astron. Soc., 496, L28, doi: [10.1093/mnrasl/slaa070](https://doi.org/10.1093/mnrasl/slaa070)
- Li, Z.-X., Gao, H., Ding, X.-H., Wang, G.-J., & Zhang, B. 2018, Nature Commun., 9, 3833, doi: [10.1038/s41467-018-06303-0](https://doi.org/10.1038/s41467-018-06303-0)
- Liu, Y., Zhang, Y., Yu, H., & Wu, P. 2025. <https://arxiv.org/abs/2506.03536>
- Lorimer, D. R., Bailes, M., McLaughlin, M. A., Narkevic, D. J., & Crawford, F. 2007, Science, 318, 777–780, doi: [10.1126/science.1147532](https://doi.org/10.1126/science.1147532)
- Macquart, J. P., et al. 2020, Nature, 581, 391, doi: [10.1038/s41586-020-2300-2](https://doi.org/10.1038/s41586-020-2300-2)
- Mastrogiovanni, S., Leyde, K., Karathanasis, C., et al. 2021, Phys. Rev. D, 104, 062009, doi: [10.1103/PhysRevD.104.062009](https://doi.org/10.1103/PhysRevD.104.062009)
- Mastrogiovanni, S., Laghi, D., Gray, R., et al. 2023, Phys. Rev. D, 108, 042002, doi: [10.1103/PhysRevD.108.042002](https://doi.org/10.1103/PhysRevD.108.042002)
- Mastrogiovanni, S., Pierra, G., Perriès, S., et al. 2024, Astron. Astrophys., 682, A167, doi: [10.1051/0004-6361/202347007](https://doi.org/10.1051/0004-6361/202347007)
- Masui, K. 2023, Nature Astronomy, 7, 749, doi: [10.1038/s41550-023-01970-6](https://doi.org/10.1038/s41550-023-01970-6)
- McQuinn, M. 2013, The Astrophysical Journal Letters, 780, L33, doi: [10.1088/2041-8205/780/2/L33](https://doi.org/10.1088/2041-8205/780/2/L33)
- Michilli, D., Bhardwaj, M., Brar, C., et al. 2023, ApJ, 950, 134, doi: [10.3847/1538-4357/accf89](https://doi.org/10.3847/1538-4357/accf89)
- Muttoni, N., Laghi, D., Tamanini, N., Marsat, S., & Izquierdo-Villalba, D. 2023, Phys. Rev. D, 108, 043543, doi: [10.1103/PhysRevD.108.043543](https://doi.org/10.1103/PhysRevD.108.043543)
- Ostriker, J. P., & Steinhardt, P. J. 1995, Nature, 377, 600, doi: [10.1038/377600a0](https://doi.org/10.1038/377600a0)
- Prochaska, J. X., & Zheng, Y. 2019, Monthly Notices of the Royal Astronomical Society, 485, 648, doi: [10.1093/mnras/stz261](https://doi.org/10.1093/mnras/stz261)
- Prochaska, J. X., Macquart, J.-P., McQuinn, M., et al. 2019, Science, 366, 231, doi: [10.1126/science.aay0073](https://doi.org/10.1126/science.aay0073)
- Qiang, D.-C., & Wei, H. 2020, JCAP, 04, 023, doi: [10.1088/1475-7516/2020/04/023](https://doi.org/10.1088/1475-7516/2020/04/023)
- Qiang, D.-C., You, Z., Yang, S., Zhu, Z.-H., & Chen, T.-W. 2025, Astrophys. J., 979, 95, doi: [10.3847/1538-4357/ada28c](https://doi.org/10.3847/1538-4357/ada28c)
- Qiu, X.-W., Zhao, Z.-W., Wang, L.-F., Zhang, J.-F., & Zhang, X. 2022, JCAP, 02, 006, doi: [10.1088/1475-7516/2022/02/006](https://doi.org/10.1088/1475-7516/2022/02/006)
- Rajwade, K. M., Driessen, L. N., Barr, E. D., et al. 2024, MNRAS, 532, 3881, doi: [10.1093/mnras/stae1652](https://doi.org/10.1093/mnras/stae1652)
- Ravi, V., Catha, M., D'Addario, L., et al. 2019, Nature, 572, 352, doi: [10.1038/s41586-019-1389-7](https://doi.org/10.1038/s41586-019-1389-7)
- Ravi, V., Law, C. J., Li, D., et al. 2022, MNRAS, 513, 982, doi: [10.1093/mnras/stac465](https://doi.org/10.1093/mnras/stac465)
- Riess, A. G., et al. 2022, Astrophys. J. Lett., 934, L7, doi: [10.3847/2041-8213/ac5c5b](https://doi.org/10.3847/2041-8213/ac5c5b)
- Ryder, S. D., Bannister, K. W., Bhandari, S., et al. 2023, Science, 382, 294, doi: [10.1126/science.adf2678](https://doi.org/10.1126/science.adf2678)
- Schutz, B. F. 1986, Nature, 323, 310, doi: [10.1038/323310a0](https://doi.org/10.1038/323310a0)
- Shannon, R. M., Bannister, K. W., Bera, A., et al. 2025, Publ. Astron. Soc. Aust., 42, e036, doi: [10.1017/pasa.2025.8](https://doi.org/10.1017/pasa.2025.8)
- Sharma, K., Ravi, V., Connor, L., et al. 2024, Nature, 635, 61, doi: [10.1038/s41586-024-08074-9](https://doi.org/10.1038/s41586-024-08074-9)
- Shin, K., Leung, C., Simha, S., et al. 2024, arXiv e-prints, arXiv:2410.07307, doi: [10.48550/arXiv.2410.07307](https://doi.org/10.48550/arXiv.2410.07307)
- Shull, J. M., Smith, B. D., & Danforth, C. W. 2012, Astrophys. J., 759, 23, doi: [10.1088/0004-637X/759/1/23](https://doi.org/10.1088/0004-637X/759/1/23)
- Song, J.-Y., Qi, J.-Z., Zhang, J.-F., & Zhang, X. 2025, Astrophys. J. Lett., 985, L44, doi: [10.3847/2041-8213/add999](https://doi.org/10.3847/2041-8213/add999)
- Song, J.-Y., Wang, L.-F., Li, Y., et al. 2024, Sci. China Phys. Mech. Astron., 67, 230411, doi: [10.1007/s11433-023-2260-2](https://doi.org/10.1007/s11433-023-2260-2)
- Taylor, S. R., Gair, J. R., & Mandel, I. 2012, Phys. Rev. D, 85, 023535, doi: [10.1103/PhysRevD.85.023535](https://doi.org/10.1103/PhysRevD.85.023535)
- Tendulkar, S. P., Bassa, C. G., Cordes, J. M., et al. 2017, ApJL, 834, L7, doi: [10.3847/2041-8213/834/2/L7](https://doi.org/10.3847/2041-8213/834/2/L7)
- Thornton, D., Stappers, B., Bailes, M., et al. 2013, Science, 341, 53–56, doi: [10.1126/science.1236798](https://doi.org/10.1126/science.1236798)

- Tian, J., Rajwade, K. M., Pastor-Marazuela, I., et al. 2024, Mon. Not. Roy. Astron. Soc., 533, 3174, doi: [10.1093/mnras/stae2013](https://doi.org/10.1093/mnras/stae2013)
- Wang, B., & Wei, J.-J. 2023, Astrophys. J., 944, 50, doi: [10.3847/1538-4357/acb2c8](https://doi.org/10.3847/1538-4357/acb2c8)
- Wang, L.-F., Jin, S.-J., Zhang, J.-F., & Zhang, X. 2022, Sci. China Phys. Mech. Astron., 65, 210411, doi: [10.1007/s11433-021-1736-6](https://doi.org/10.1007/s11433-021-1736-6)
- Wang, L.-F., Zhang, X.-N., Zhang, J.-F., & Zhang, X. 2018, Phys. Lett. B, 782, 87, doi: [10.1016/j.physletb.2018.05.027](https://doi.org/10.1016/j.physletb.2018.05.027)
- Wang, L.-F., Zhao, Z.-W., Zhang, J.-F., & Zhang, X. 2020, JCAP, 11, 012, doi: [10.1088/1475-7516/2020/11/012](https://doi.org/10.1088/1475-7516/2020/11/012)
- Wang, Y.-Y., Gao, S.-J., & Fan, Y.-Z. 2025, Astrophys. J., 981, 9, doi: [10.3847/1538-4357/adade8](https://doi.org/10.3847/1538-4357/adade8)
- Wei, J.-J., Wu, X.-F., & Gao, H. 2018, Astrophys. J. Lett., 860, L7, doi: [10.3847/2041-8213/aac8e2](https://doi.org/10.3847/2041-8213/aac8e2)
- Wu, P.-J., Shao, Y., Jin, S.-J., & Zhang, X. 2023, JCAP, 06, 052, doi: [10.1088/1475-7516/2023/06/052](https://doi.org/10.1088/1475-7516/2023/06/052)
- Wu, Q., & Wang, F.-Y. 2024, Chin. Phys. Lett., 41, 119801, doi: [10.1088/0256-307X/41/11/119801](https://doi.org/10.1088/0256-307X/41/11/119801)
- Wu, Q., Zhang, G.-Q., & Wang, F.-Y. 2022, Mon. Not. Roy. Astron. Soc., 515, L1, doi: [10.1093/mnrasl/slac022](https://doi.org/10.1093/mnrasl/slac022)
- Xiao, S.-R., Shao, Y., Wang, L.-F., et al. 2024, <https://arxiv.org/abs/2408.00609>
- Yang, K. B., Wu, Q., & Wang, F. Y. 2022, Astrophys. J. Lett., 940, L29, doi: [10.3847/2041-8213/aca145](https://doi.org/10.3847/2041-8213/aca145)
- Yang, T.-C., Hashimoto, T., Hsu, T.-Y., et al. 2025, Astron. Astrophys., 693, A85, doi: [10.1051/0004-6361/202450823](https://doi.org/10.1051/0004-6361/202450823)
- Yu, J., Liu, Z., Yang, X., et al. 2024, Astrophys. J. Suppl., 270, 24, doi: [10.3847/1538-4365/ad0ece](https://doi.org/10.3847/1538-4365/ad0ece)
- Yu, J., Wang, Y., Zhao, W., & Lu, Y. 2020, Mon. Not. Roy. Astron. Soc., 498, 1786, doi: [10.1093/mnras/staa2465](https://doi.org/10.1093/mnras/staa2465)
- Yun, Q., Han, W.-B., Hu, Q., & Xu, H. 2023, Mon. Not. Roy. Astron. Soc., 527, L60, doi: [10.1093/mnrasl/slad119](https://doi.org/10.1093/mnrasl/slad119)
- Zhang, G. Q., Yu, H., He, J. H., & Wang, F. Y. 2020, Astrophys. J., 900, 170, doi: [10.3847/1538-4357/abaa4a](https://doi.org/10.3847/1538-4357/abaa4a)
- Zhang, J.-F., Zhang, M., Jin, S.-J., Qi, J.-Z., & Zhang, X. 2019a, JCAP, 09, 068, doi: [10.1088/1475-7516/2019/09/068](https://doi.org/10.1088/1475-7516/2019/09/068)
- Zhang, J.-G., Jiang, Y.-F., Zhao, Z.-W., et al. 2025a, Sci. China Phys. Mech. Astron., 68, 280406, doi: [10.1007/s11433-024-2647-2](https://doi.org/10.1007/s11433-024-2647-2)
- Zhang, J.-G., Zhao, Z.-W., Li, Y., et al. 2023, Sci. China Phys. Mech. Astron., 66, 120412, doi: [10.1007/s11433-023-2212-9](https://doi.org/10.1007/s11433-023-2212-9)
- Zhang, X. 2019, Sci. China Phys. Mech. Astron., 62, 110431, doi: [10.1007/s11433-019-9445-7](https://doi.org/10.1007/s11433-019-9445-7)
- Zhang, X.-N., Wang, L.-F., Zhang, J.-F., & Zhang, X. 2019b, Phys. Rev. D, 99, 063510, doi: [10.1103/PhysRevD.99.063510](https://doi.org/10.1103/PhysRevD.99.063510)
- Zhang, Y., Liu, Y., Yu, H., & Wu, P. 2025b, <https://arxiv.org/abs/2504.06845>
- Zhang, Z. J., Yan, K., Li, C. M., Zhang, G. Q., & Wang, F. Y. 2021, Astrophys. J., 906, 49, doi: [10.3847/1538-4357/abceb9](https://doi.org/10.3847/1538-4357/abceb9)
- Zhang, Z.-L., & Zhang, B. 2025, Astrophys. J. Lett., 984, L40, doi: [10.3847/2041-8213/adcc30](https://doi.org/10.3847/2041-8213/adcc30)
- Zhao, W., Van Den Broeck, C., Baskaran, D., & Li, T. G. F. 2011, Phys. Rev. D, 83, 023005, doi: [10.1103/PhysRevD.83.023005](https://doi.org/10.1103/PhysRevD.83.023005)
- Zhao, Z.-W., Li, Z.-X., Qi, J.-Z., et al. 2020a, Astrophys. J., 903, 83, doi: [10.3847/1538-4357/abb8ce](https://doi.org/10.3847/1538-4357/abb8ce)
- Zhao, Z.-W., Wang, L.-F., Zhang, J.-F., & Zhang, X. 2020b, Sci. Bull., 65, 1340, doi: [10.1016/j.scib.2020.04.032](https://doi.org/10.1016/j.scib.2020.04.032)
- Zheng, J., Liu, X.-H., & Qi, J.-Z. 2024, Astrophys. J., 975, 215, doi: [10.3847/1538-4357/ad7bb5](https://doi.org/10.3847/1538-4357/ad7bb5)
- Zhou, B., Li, X., Wang, T., Fan, Y.-Z., & Wei, D.-M. 2014, Phys. Rev. D, 89, 107303, doi: [10.1103/PhysRevD.89.107303](https://doi.org/10.1103/PhysRevD.89.107303)
- Zhu, L.-G., Fan, H.-M., Chen, X., Hu, Y.-M., & Zhang, J.-d. 2024, Astrophys. J. Suppl., 273, 24, doi: [10.3847/1538-4365/ad5446](https://doi.org/10.3847/1538-4365/ad5446)
- Zhu, L.-G., Hu, Y.-M., Wang, H.-T., et al. 2022a, Phys. Rev. Res., 4, 013247, doi: [10.1103/PhysRevResearch.4.013247](https://doi.org/10.1103/PhysRevResearch.4.013247)
- Zhu, L.-G., Xie, L.-H., Hu, Y.-M., et al. 2022b, Sci. China Phys. Mech. Astron., 65, 259811, doi: [10.1007/s11433-021-1859-9](https://doi.org/10.1007/s11433-021-1859-9)